UDC 539.4

Study on Non-Linear Flexural Behavior of Reinforced Concrete Beams Using ANSYS by Discrete Reinforcement Modeling

G. Vasudevan,[a] S. Kothandaraman,[b] and S. Azhagarsamy[b]

[a] Perunthalaivar Kamarajar Institute of Engineering and Technology, Karaikal, India

[b] Pondicherry Engineering College, Puducherry, India

УДК 539.4

Исследование характеристик нелинейного изгиба железобетонных балок путем дискретного моделирования армирования с помощью программного пакета ANSYS

Г. Васудеван[а], С. Котхандараман[б], С. Ажагарсами[б]

[а] Механико-технологический институт им. Перунтхалаивара Камараяра, Караикал, Индия

[б] Технический колледж г. Пудучерри, Индия

Рассматриваются экспериментальные данные по четырехточечному изгибу шести железобетонных балок и конечноэлементные расчетные результаты дискретного моделирования армирования, полученные с помощью программного пакета ANSYS 12.0. Критические значения экспериментальных характеристик сравниваются с аналитическими решениями на основании стандарта IS 456: 2000. Графическое представление большого объема расчетных результатов, включая конфигурацию изогнутой балки, изменение напряженно-деформированного состояния по ее длине и глубине, а также кинетику роста трещин, осуществляется с помощью батч-файла, написанного на языке программирования ANSYS APDL. Сравнительный анализ экспериментальных, конечноэлементных и аналитических результатов проводится для случаев формирования исходной трещины в балках и для критической несущей способности балок с целью детального изучения их поведения и минимизации объема последующих испытаний до разрушения в лабораторных условиях.

Ключевые слова: пакет ANSYS, язык программирования APDL, растрескивание, текучесть, нелинейный и критический изгиб, прогиб балки.

Introduction. The non-linear behavior of reinforced concrete (RC) beams till ultimate failure is a complicated phenomenon due to the involvement of heterogenic material properties and cracking behavior of concrete. Behavior prediction of reinforced concrete elements till failure are usually carried out using experimental testing and the observations are recorded only at critical locations due to restriction in cost of testing equipments and accessories. In order to avoid the destructive testing, reduction of the cost of materials and manpower, the behavior prediction of RC beams are generally carried out using numerical methods. Though enormous research is already carried out on the non-linear finite element analysis (FEA) of RC beams, a considerable effort is made in this study to effectively utilize the

ANSYS to validate the experimental results and generate wide range of graphical display of the results which may even difficult to ascertain by experimental testing due to the reasons stated above. FE analysis was carried out using IS 456: 2000 [1] guidelines for material modeling of concrete and steel. The critical values of the test and FEA results such as initial cracking and ultimate moment were compared with calculated values as per IS 456: 2000 [1] codal provisions.

1. **Review of Literature**. Experimental testing on the flexural behavior of RC beams has been carried out by Buckhouse [2] and the critical results were compared with analytical values. Wolanski [3] has carried out the FEA using ANSYS on the experimental beams provided by Buckhouse [2] and validated the results. He has used Solid65, Solid45, and Link8 elements to model concrete, steel cushion at the supports and loading points with one quarter of the beam model. The steel reinforcements were incorporated in the concrete elements through the nodes created by the mesh of the concrete volume. Boundary conditions were applied at points of symmetry, and at the supports. Kachlakev, et al. [4] studied the behavior of RC beams with externally bonded carbon fiber reinforced polymer (CFRP) fabric using ANSYS. They followed smeared cracking approach for FE modeling using Solid65 for concrete, Link8 for rebar, Solid46 for FRP composites and Solid45 for steel plates at the supports and loading points. They stated that the use of ANSYS to model RC beam with FRP composites was viable and the results were in good agreement with experimental testing. Fanning [5] tested and analysed two numbers of $155 \times 240 \times 3000$ mm long RC beams and found that the results of the FE models were sensitive to the Young modulus of the concrete and the yield strength of the reinforcement. Dahmani et al. [6], studied the crack propagation in RC beams using ANSYS modelled with Solid65 element with smeared reinforcement approach, in which the concrete and the reinforcing were incorporated into elements with the same geometrical boundaries and the effects of reinforcing were averaged within the pertaining element. Based on the results, they stated that, in spite of the relative simplicity of the employed models, satisfactory predictions of the response were obtained. Travarez [7] discussed the merits and demerits of discrete model, embedded model and smeared model for incorporating reinforcements depending on the type of system. Vasudevan and Kothandaraman [8] explored the advantages of batch mode for FEA of concrete beams.

Preliminary comparative study by test, FEA and analytical method was conducted by Vasudevan and Kothandaraman [9] with regards to initial cracking and ultimate behavior using one quarter of the beam for three beam specimens and found that the results are in good agreement.

2. **Beam Specimens Used for the Study**. Six numbers of beam specimens with two grades of concrete designated as N and H with targeted cube compressive strength of 30 and 40 MPa was used for experimental and finite element analysis. Beam specimens of size $2000 \times 250 \times 200$ mm with an effective span of 1800 mm was used for the study. Tension bars of 2 numbers 10, 12, and 16 mm diameter, hanger bars of 2 numbers of 10 mm diameters and shear reinforcement of two legged 8 mm diameter at 200 mm spacing were used for the present study. The clear cover of 25 mm was used in the experimental testing and effective cover 31.25 mm was used for FE modeling for all the beam specimens. The beams were tested for four-point bending with loading at a distance of 550 mm from either end

of the support, so as to have a moment span of 700 mm. All the beam specimens were analysed using ANSYS 12.0 based on the material properties and multi-linear stress–strain curve for concrete provided by IS 456: 2000 [1] and from the literatures [3–7]. All other parameters which are not discussed in this paper were considered as default values from ANSYS. The details and other parameters used for the study are shown in Fig. 1 and Table 1.

T a b l e 1

Details of Beams

No.	Beam specimen	Concrete			Steel reinforcement		
		f_{ck}, MPa	f_{cr}, MPa	E_c, MPa	Numbers/ Diameter	f_Y, MPa	Percentage p_t, %
1	RF-N-10	35.6	4.18	29,833	2/10 mm	556	0.36
2	RF-N-12	35.8	4.19	29,917	2/12 mm	525	0.52
3	RF-N-16	33.4	4.05	28,896	2/16 mm	522	0.92
4	RF-H-10	45.2	4.71	33,615	2/10 mm	556	0.36
5	RF-H-12	45.8	4.74	33,838	2/12 mm	525	0.52
6	RF-H-16	48.3	4.86	34,749	2/16 mm	522	0.92

Note. f_{ck} is the cube compressive strength; f_{cr} is the modulus of rupture, $f_{cr} = 0.7\sqrt{f_{ck}}$ [1]; E_c is the modulus of elasticity, $E_c = 5000\sqrt{f_{ck}}$ [1]; f_Y is the yield strength of steel.

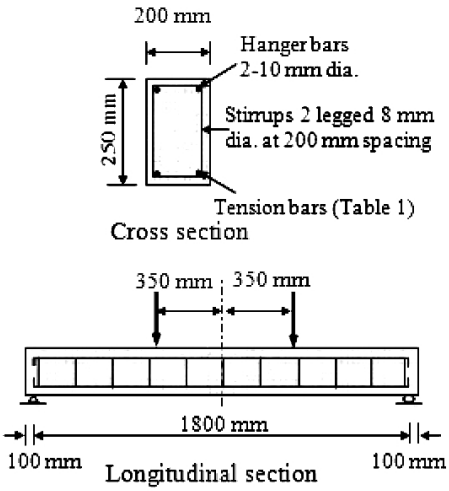

Fig. 1. Beam specimen.

3. **Experimental Investigation**. The beams were tested in flexure using a loading frame and a hydraulic jack of capacities 300 and 500 kN, respectively. The two-point loading was applied through a spreader beam with a constant-moment zone of 700 mm. Specimens were supported on a pair of steel hinge-roller supports with a clear span of 1800 mm. The deflections were recorded at the mid-span and at the loading points using LVDTs connected to a data-logger and a computer. Concrete surface strains at both of the side faces of the beams were recorded at six locations along the depth of the beam. Loading was applied gradually through the

hydraulic jack. The beams were loaded to a maximum deflection of around 25 mm or up to the formation of crack of width 5 mm or till the crushing of concrete. Tests were terminated after beam attains the ultimate failure by any of the failure mode. During the loading process, developments of cracks were observed at every 5 kN and the pattern of cracks were drawn on the beam. Load at the formation of first crack was also observed and recorded. The test setup used in the investigation is shown in Fig. 2.

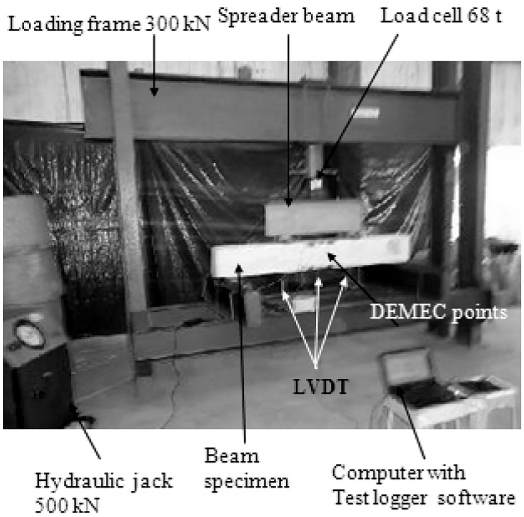

Fig. 2. Experimental setup.

4. **Finite Element Analysis using ANSYS**. RC beam specimens were modelled using eight noded Solid65 element with three degrees of freedom at each node (translations in the nodal x, y, and z directions), capable of handling nonlinear behavior, cracking in three orthogonal directions due to tension, crushing in compression and plastic deformation. The reinforcing bars were incorporated in the concrete model using two noded Link8 spar element with three degrees of freedom at each node (translations in the nodal x, y, and z directions), capable of handling plasticity, creep, swelling, stress stiffening and large deflection. The supports and loading points were modelled as steel cushion to avoid stress concentration problem using eight noded Solid45 element with three degrees of freedom at each node (translations in the nodal x, y, and z directions), which handles plasticity, creep, swelling, stress stiffening, large deflection and strain. One-quarter of the beam was modelled for the FEA by using the appropriate boundary conditions due to symmetry as shown in Fig. 3. Material model for concrete used for the study is derived from IS 456: 2000 [1] with a partial safety factor of 1.0. Other parameters used for the modeling is furnished in Tables 1 and 2. Parameters which are not stated in this report were taken as program default. The FE modeling was carried out in batch mode in sequence using, KEYPOINTS, LINES, LESIZE, VOLUME, VMESH and VSWEEP commands. The rebar elements were introduced in the nodes of the concrete elements using discrete reinforcement modeling which is most preferred for RC elements with well defined reinforcement locations using E and EGEN commands. The support conditions were created using displacement (D)

boundary conditions. The entire process of the non-linear finite element analysis such as geometrical modeling, material modeling, parameters for non-linear analysis, creation of load-steps, graphical post processing of results, generation of various graphs and images and output in the form of text file was generated using a single input file developed using the ANSYS parametric design language (APDL) [10]. The FE model with discrete reinforcement model is shown in Fig. 4.

T a b l e 2

Materials Properties for Concrete and Steel

Yield strength of hanger bars	556 MPa	Shear transfer coefficient for open crack	0.3
Yield strength of stirrups	550 MPa	Shear transfer coefficient for closed crack	1.0
Tangent modulus for steel	20 MPa	Uniaxial crushing stress value	−1.0
Poisson's ratio of concrete	0.2	Stiffness multiplier constant (T_c)	0.6
Poisson's ratio of steel	0.3		

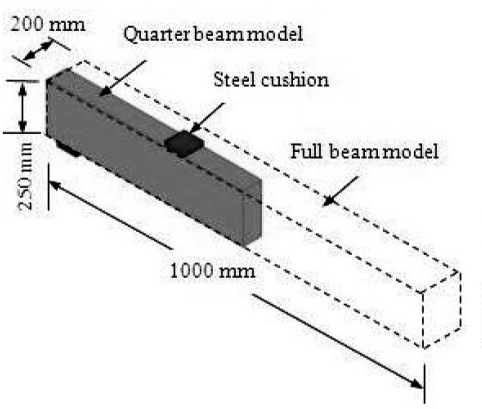

Fig. 3. Quarter beam model.

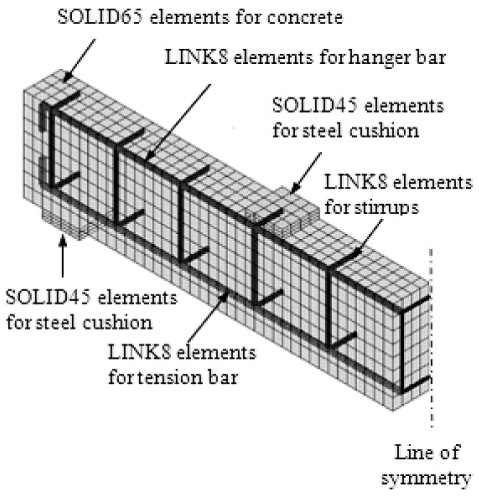

Fig. 4. FE model with reinforcement.

5. **Results and Discussion**.

5.1. ***Load–Deflection Behavior***. Plots of load versus mid-span and load-point deflections from experiment and FEA are shown in Fig. 5 for beams in N and H series. The shape of the load–deflection plots are trilinear and immediately after the first crack formation, there is a small kink in the FEA plot, which is due to sudden loss of moment of inertia after the first crack formation. For beams with higher percentage of reinforcement, the variation of deflection is less when compared to beams with lower percentage of reinforcement. This is due to the fact that, the loss of moment of inertia due to crack formation for beams with higher percentage of reinforcement is less than the beams with lower percentage of reinforcement. Also, the comparison with experimental and FEA curves indicated that the experimental and FEA results are in good agreement.

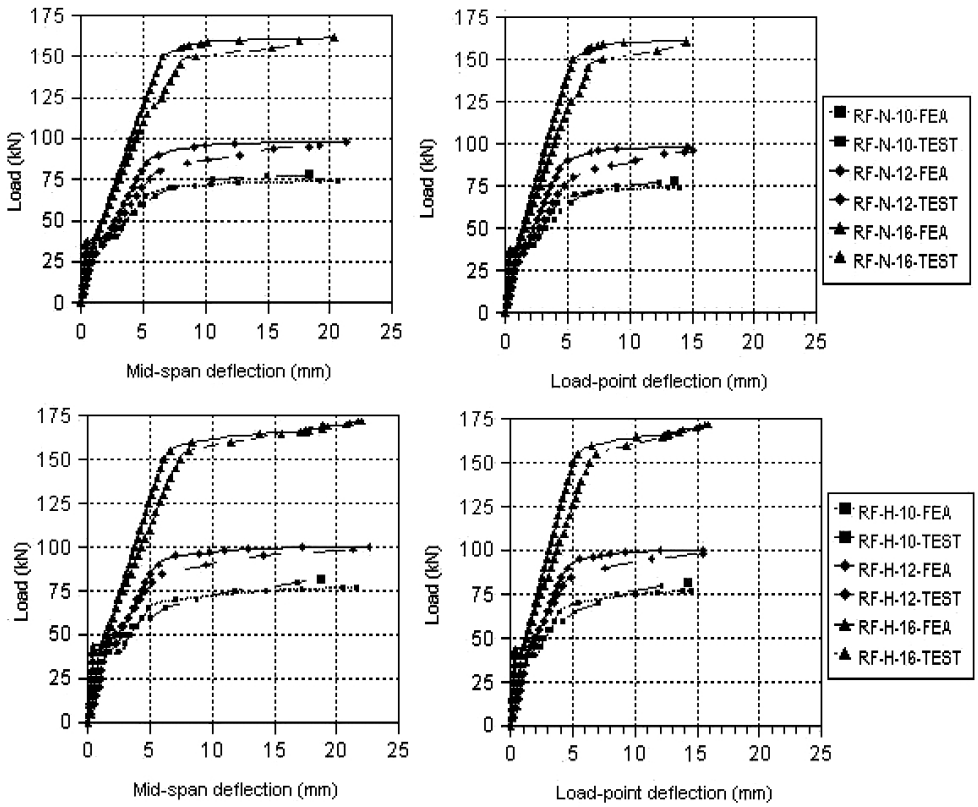

Fig. 5. Load–deflection behavior.

5.2. ***Deflected Shape of the Beam at Various Loading Stages***. The deflected profile of the beam along the span also clearly depicts the three stages of the load–deflection curves as shown in Fig. 6. It is noted that the sudden increase in deflection immediately after the formation of first crack and steel yielding stage clearly reflects the kinks of the trilinear load–deflection behavior as depicted in Fig. 5.

5.3. ***Load–Strain Behavior***. Strain values at the soffit and at the top compression face of the beam were recorded from experimental testing and are compared with FEA results. The plots of load versus compressive strain at the top surface of beam and tensile strain at the soffit level at the mid-span section are depicted as shown in Fig. 7 for beam specimens in N and H series. The load versus compressive strain for the top compression face of the beams obtained by FEA is in good agreement with the experimental results. However, the concrete tensile strain measurements by obtained by experiment and FEA are greatly influenced by the cracking of concrete and hence the values seem to be inconsistent as shown in Fig. 7.

5.4. ***Strain Variation along the Length of the Beam at Various Stages***. In order to have a better understanding of the strain distribution due to four-point bending, the variation of strain along the length of the beam were generated for various loading increments and are depicted in Fig. 8. The strain variation along the length of the beam clearly indicates peak values at the mid-span section. It is

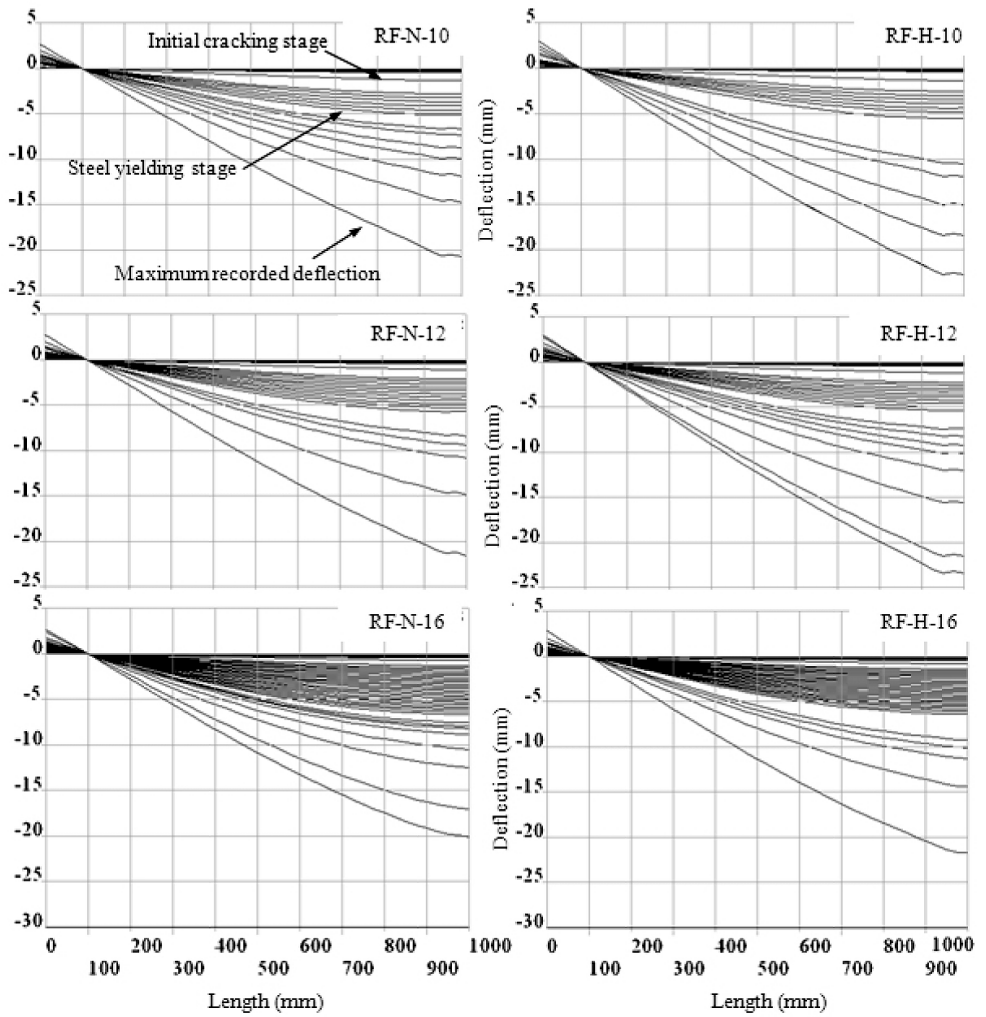

Fig. 6. Deflected profile of the beams at various loading stages.

also seen that, at the loading points, the strain values are less due to the local stiffness contributed by the provision of additional steel cushions.

5.5. ***Load–Stress Behavior***. Stress distribution along the depth of the beam at mid-span section for beam specimens in N and H series are plotted as shown in Fig. 9. The variation of stress along the depth of beam clearly indicates the gradual shifting of neutral axis towards the compression face of the beam during the process of crack propagation. The stress distribution at the compression face and at the soffit levels of the concrete are generated along the length of the beam by ANSYS and are furnished in Fig. 10. The stress distribution at the compression face of the concrete represents peak values at the mid-span section of the beam with considerable drop in the magnitude of the stresses at the loading points due additional stiffness contributed by the provision of steel cushion. The tensile stresses in concrete at the soffit level shows uniform distribution due to the transfer of tensile stress to the tension reinforcement and are in the range of modulus of rupture of concrete.

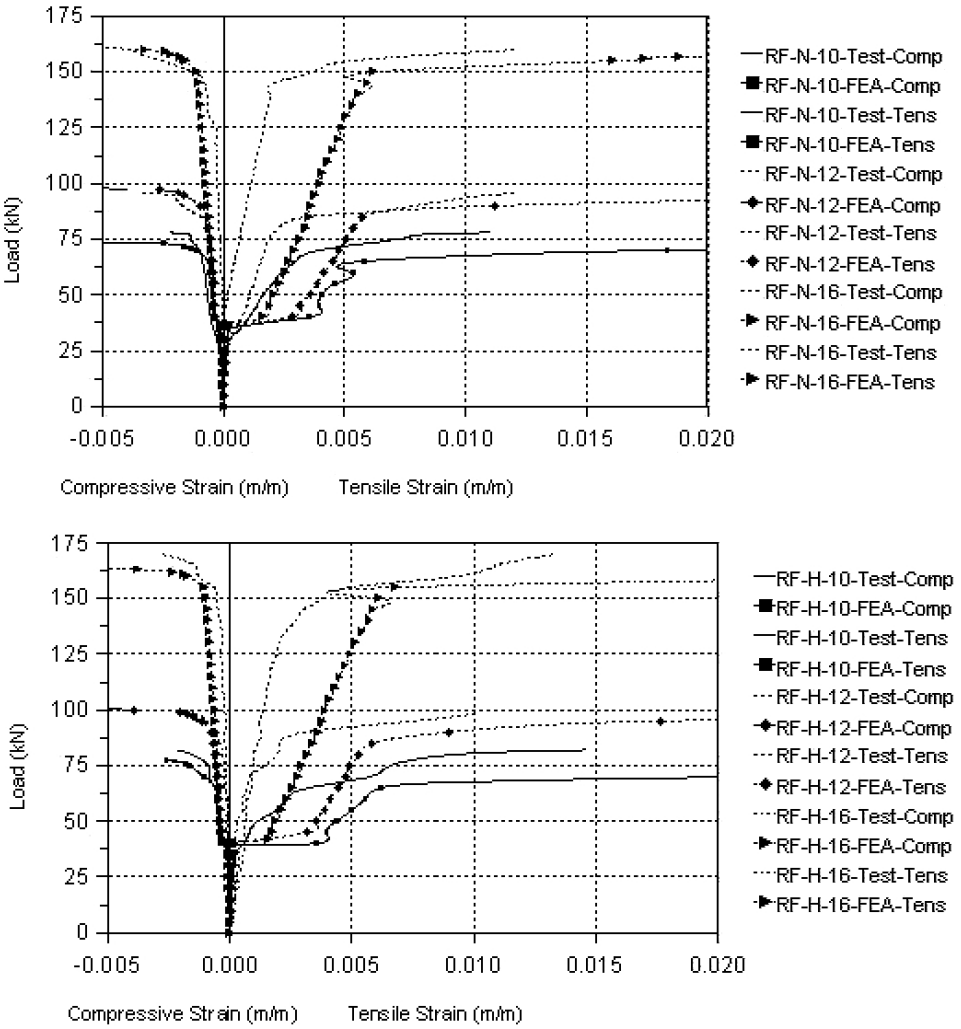

Fig. 7. Load–strain behavior.

5.6. ***Crack Formation***. Crack patterns developed during the experimental testing were keenly observed and marked on the beam and compared with cracking regions generated by FEA and are presented in Fig. 11, which gives clear picture of the four point bending behavior of the beams. It is to be noted that the crack patterns generated by ANSYS are not the actual cracks but, the possible cracking regions.

5.7. ***Initial Cracking Behavior***. Though the initial cracking behavior of the beams are mainly depends on the grade of concrete, small improvement in the initial cracking behavior is seen due to increase in area of tension reinforcement. A graphical comparison of the initial cracking moment obtained by test, FEA and IS 456: 2000 [1] is presented in Fig. 12.

5.8. ***Ultimate Behavior***. Moment values observed at ultimate stage by experimental testing and obtained by FEA is compared with the analytical ultimate moment values calculated using IS 456: 2000 [1] and is depicted in Fig. 13.

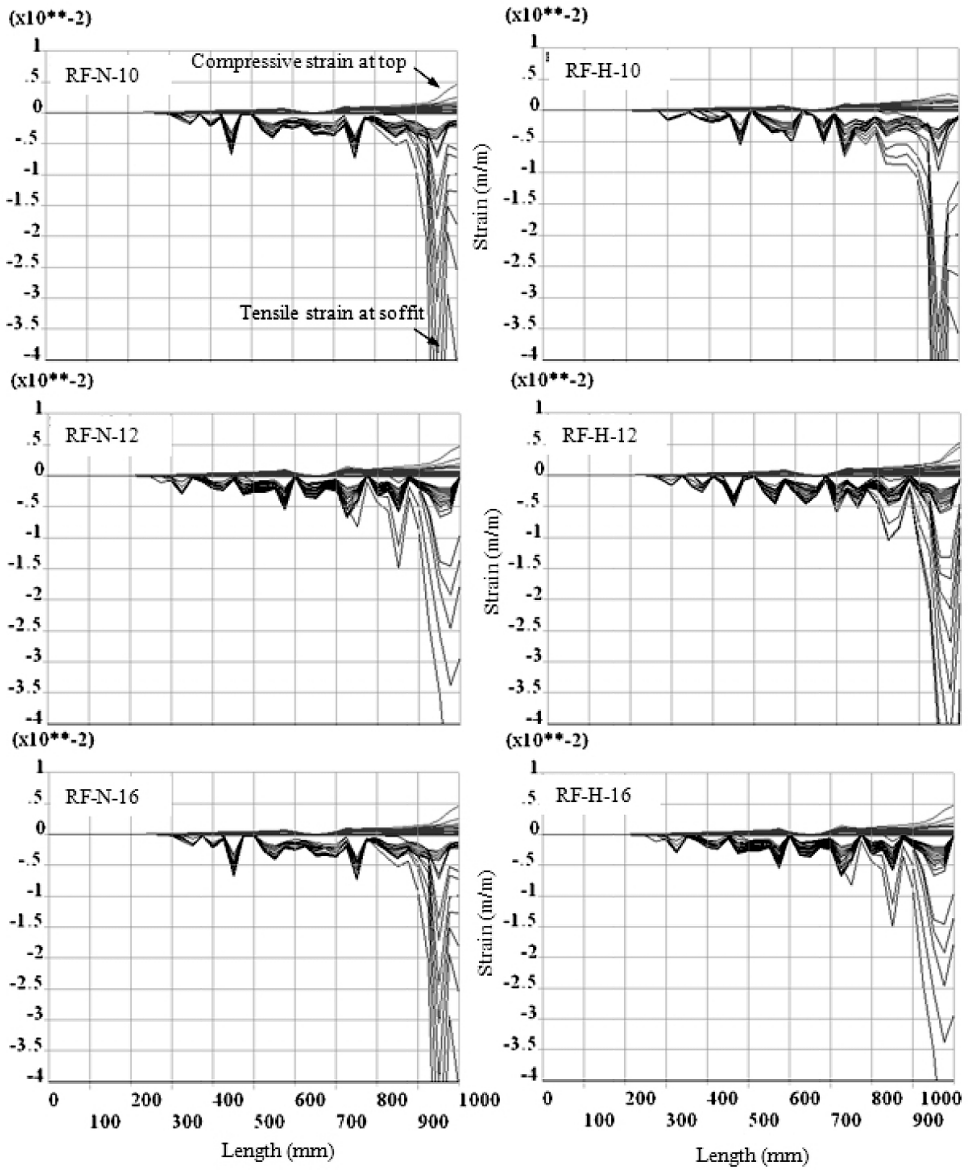

Fig. 8. Strain distribution along the length of the beams at various loading stages.

6. **Analytical Evaluation Based on IS 456: 2000**. The moment at the formation of initial crack was obtained using the moment of inertia of the transformed section using Eq. (1).

$$\text{Moment at initial crack, } M_{cr} = \frac{f_{cr} I_{tr}}{y_b}. \tag{1}$$

The ultimate moment was obtained using the expressions provided in IS 456: 2000 [1] by taking the partial safety factor for concrete and steel as 1.0 using Eqs. (2) and (3).

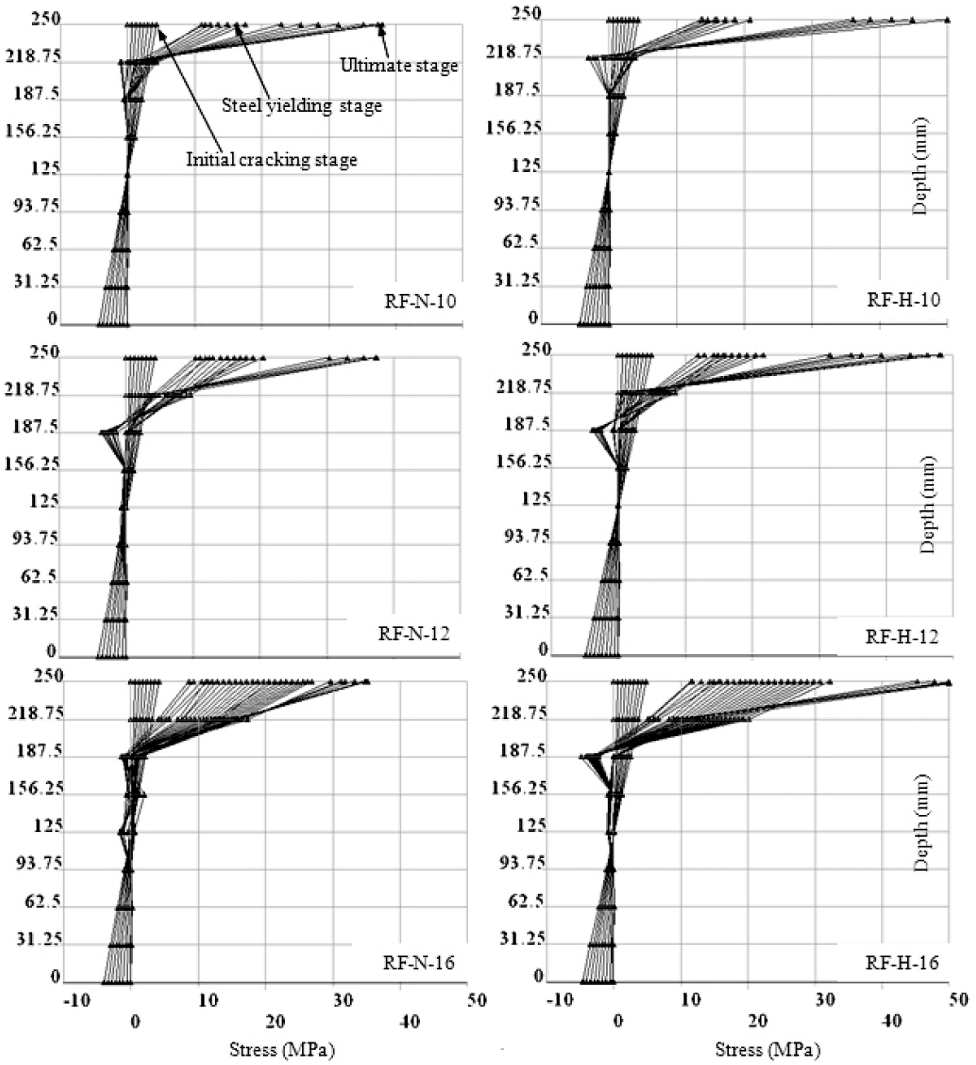

Fig. 9. Stress distribution along the depth of the beams at various loading stages.

$$\text{Depth of neutral axis, } x_u = \frac{f_Y A_{st}}{0.542 f_{ck} b}, \tag{2}$$

$$\text{ultimate moment capacity, } M_u = A_{st} f_Y (d - 0.42 x_u), \tag{3}$$

where b is the breadth of beam (mm), d is the overall depth of beam (mm), y_b is the distance of the bottom fibre from neutral axis (mm), I_{tr} is the transformed moment of inertia of the section (mm^4), and A_{st} is the area of tension steel (mm^2).

A Visual Basic program has been developed for performing the above calculations and the graphical comparison of the analytical values with the test results and FEA are depicted in Figs. 12 and 13. The analytical and FEA values and the variation with respect to experimental values are presented in Table 3.

T a b l e 3

Comparison of Initial Cracking and Ultimate Moment

No.	Beam specimen	Moment at initial crack M_{cr}, kN·m					Ultimate moment M_u, kN·m				
		M_{cr}^{test}*	FEA		IS 456: 2000		M_u^{test}*	FEA		IS 456: 2000	
			M_{cr}^{FEA}	Δ_{cr}^{FEA}, %	M_{cr}^{IS}	Δ_{cr}^{IS}, %		M_u^{FEA}	Δ_u^{FEA}, %	M_u^{IS}	Δ_u^{IS}, %
1	RF-N-10	7.98	9.71	21.68	9.16	14.79	21.45	20.40	−4.90	18.38	−14.31
2	RF-N-12	8.80	9.94	12.95	9.37	6.48	26.40	26.95	2.08	24.48	−7.27
3	RF-N-16	9.63	10.21	6.02	9.53	−1.04	44.00	44.39	0.89	40.44	−8.09
4	RF-H-10	9.63	10.87	12.88	10.27	6.65	22.55	21.23	−5.85	18.56	−17.69
5	RF-H-12	10.18	11.15	9.53	10.52	3.34	27.12	27.64	1.92	24.81	−8.52
6	RF-H-16	11.55	11.96	3.55	11.22	−2.86	46.75	47.30	1.18	42.02	−10.12

* Values excluding the self weight of beam and spreader steel beam (which gives a moment of 0.67 kN·mm).

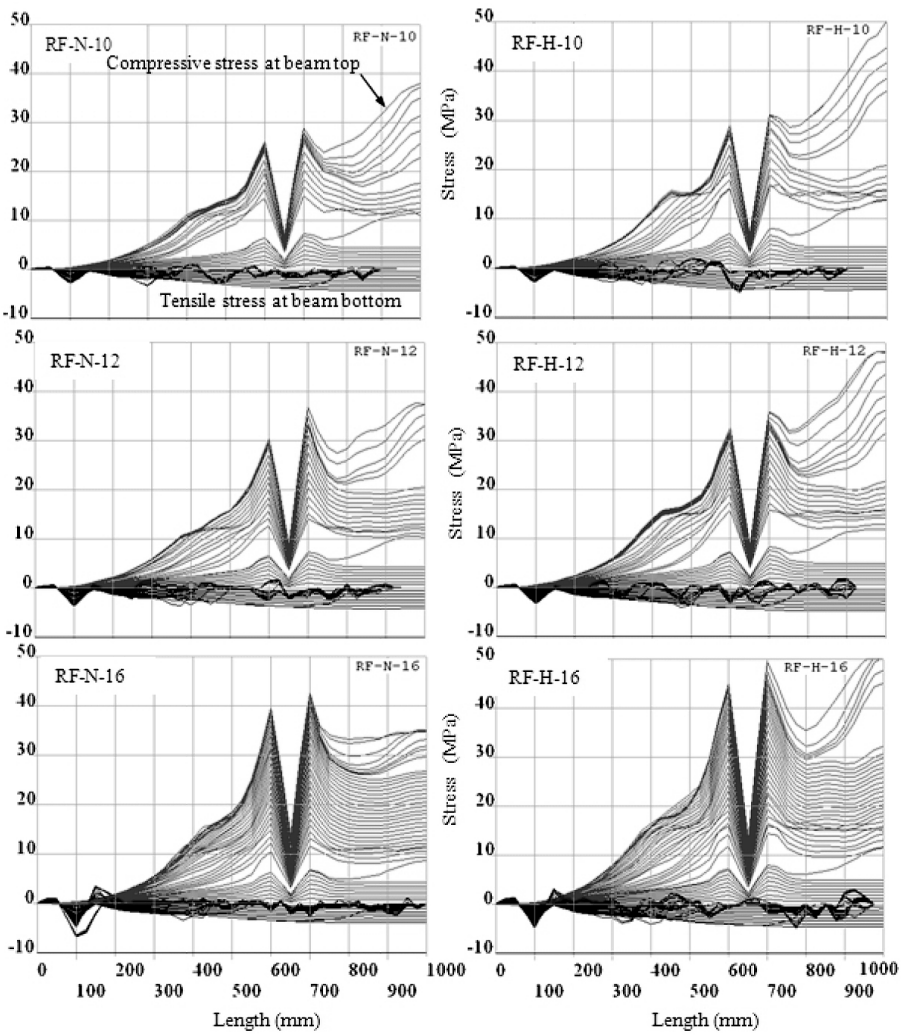

Fig. 10. Stress distribution along the length of the beams at various loading stages.

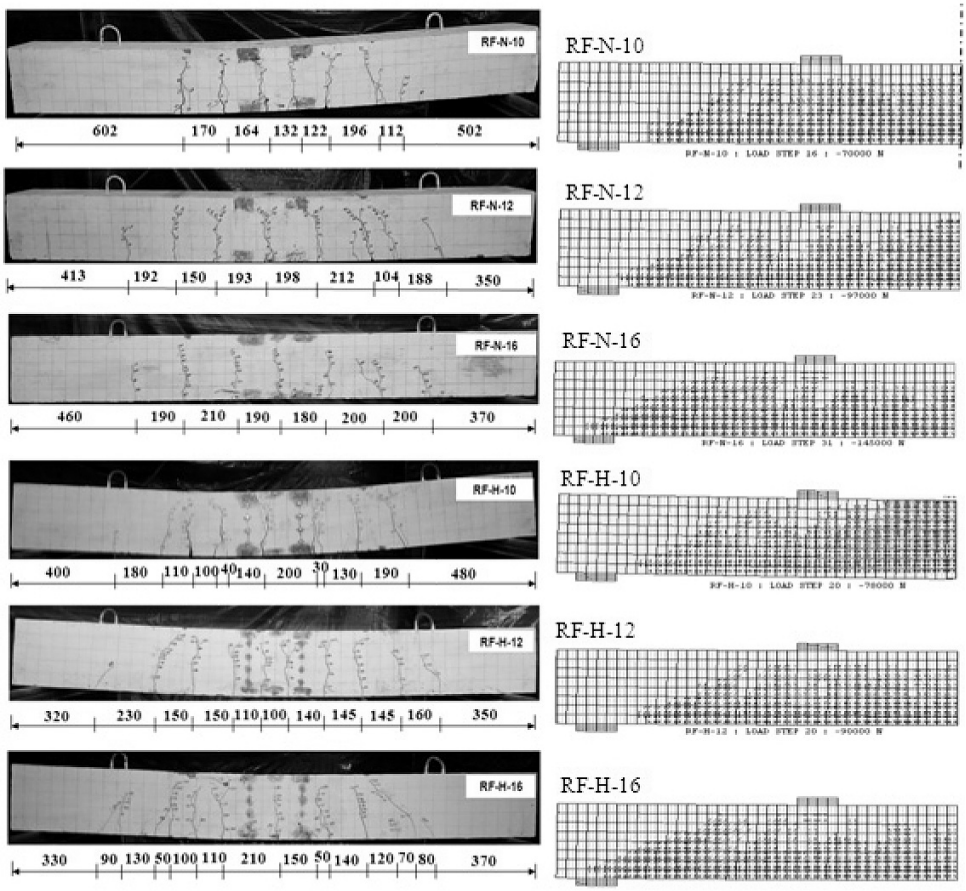

Fig. 11. Crack pattern from test and FEA.

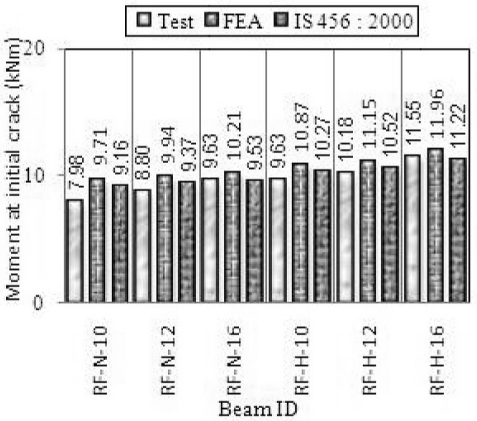

Fig. 12. Comparison of moment at initial crack.

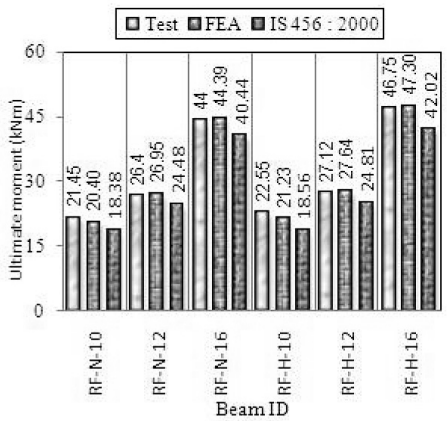

Fig. 13. Comparison of ultimate moment.

Conclusions

Based on the observation made on the experimental testing and the results of the non-linear finite element analysis (NLFEA) carried out using ANSYS by discrete reinforcement modeling on six beam specimens, the following conclusions are made.

1. Various plots constructed during FEA, such as load–deflection behavior, load–strain behavior, deflected shape, stress and strain distribution at the top compression face and at the soffit level of the beam, stress distribution along the depth of the beam generated by ANSYS gives a broader view of the non-linear behavior of RC beams.

2. Provisions of IS 456: 2000 for concrete material properties can be very well adopted for the non-linear finite element analysis using ANSYS and the results are in close agreement with experimental testing.

3. The initial cracking behavior patterns obtained by experiment, FEA and analytical calculations based on IS 456: 2000 are closely matching with each other.

4. The moment at steel yielding stage, obtained from experimental testing and FEA is closely matching with the analytical ultimate capacity calculated using IS 456: 2000 with the partial safety factor of 1.0 for concrete and steel.

5. The analytical ultimate moment capacity obtained by IS 456: 2000, is slightly lower than the tested and finite element analysis results.

6. The analysis procedure utilized in this paper and various output plots constructed by FEA have provided useful and deep insight for future application of finite element software for the non-linear analysis of RC beams.

7. Based on the large number of analysis carried out on the RC beams using ANSYS it is found that at the ultimate stage the analysis results such as deflection, rebar strain are more sensitive with respect to mesh size, materials properties, load increments, etc.

Р е з ю м е

Розглядаються експериментальні дані щодо чотириточкового згину шести залізобетонних балок і скінченноелементні розрахункові результати дискретного моделювання армування, що отримані за допомогою програмного пакета ANSYS 12.0. Критичні значення експериментальних характеристик порівнюються з аналітичними розв'язками на основі стандарту IS 456: 2000. Графічне представлення великого обсягу розрахункових результатів, включаючи конфігурацію зігнутої балки, зміну напружено-деформованого стану по її довжині і глибині та кінетику росту тріщини, проводиться за допомогою батчфайлу, написаного на мові програмування ANSYS APDL. Порівняльний аналіз експериментальних, скінченноелементних і аналітичних результатів виконано для випадків формування початкової тріщини в балках і для критичної несівної здатності балок із метою вивчення їх поведінки та мінімізації обсягу наступних випробувань до руйнування в лабораторних умовах.

1. *IS 456: 2000. Indian Standard: Plain and Reinforced Concrete – Code of Practice*, Bureau of Indian Standards, New Delhi (2000).
2. E. R. Buckhouse, *External Flexural Reinforcement of Existing Reinforced Concrete Beams Using Bolted Steel Channels*, Master of Science Thesis, Marquette University, Wisconsin (1997).
3. A. J. Wolanski, *Flexural Behavior of Reinforced and Prestressed Concrete Beams Using Finite Element Analysis*, Master of Science Thesis, Marquette University, Wisconsin (2004).

4. D. Kachlakev, T. Miller, S. Yim, et al., *Finite Element Modeling of Reinforced Concrete Structures Strengthened with FRP Laminates*, Final Report SPR 316, Oregon Department of Transportation (2001).
5. P. Fanning, "Nonlinear models of reinforced and post-tensioned concrete beams," *Electr. J. Struct. Eng.*, **2**, 111–119 (2001).
6. L. Dahmani, A. Khennane, and S. Kaci, "Crack identification in reinforced concrete beams using ANSYS software," *Strength Mater.*, **42**, No. 2, 232–240 (2010).
7. F. A. Tavarez, *Simulation of Behaviour of Composite Grid Reinforced Concrete Beams Using Explicit Finite Element Methods*, Master of Science Thesis, University of Wisconsin–Madison, Madison, Wisconsin (2001).
8. G. Vasudevan and S. Kothandaraman, "Modeling and simulation of RC beams using ANSYS by APDL batch mode approach," *CiiT Int. J. Data Min. Knowledge Eng.*, **3**, No. 11 (2011).
9. G. Vasudevan and S. Kothandaraman, "Behaviour prediction of RC beams-comparison of experimental, FEA and analytical methods," in: Proc. of the IEEE Int. Conf. on *Advances in Engineering, Science, and Management* (Nagapattinam, India, 2012), pp. 365–370.
10. *ANSYS Commands Reference*, ANSYS, http:/www.ansys.com (2005).

Received 05. 11. 2012